UC San Diego
International Symposium on Stratified Flows

Title
Intrusive gravity currents propagating into two-layer stratified ambients: Vorticity modeling

Permalink
https://escholarship.org/uc/item/2pn7t1hj

Journal
International Symposium on Stratified Flows, 1(1)

Authors
Khodkar, Mohammad Amin
Nasr-Azadani, Mohamad
Meiburg, Eckart

Publication Date
2016-08-31

Intrusive gravity currents propagating into two-layer stratified ambients: Vorticity modeling

M. A. Khodkar, M. M. Nasr-Azadani and E. Meiburg
Department of Mechanical Engineering
University of California at Santa Barbara
Santa Barbara, CA 93106.
Email: mkhodkar@umail.ucsb.edu

Abstract
A simplified model is developed for intrusive gravity currents propagating along the interface of a two-layer stratified ambient. The model is based on the conservation of mass and vorticity, and it does not require any empirical closure assumptions. A parametric study conducted with this model reproduces the correct behavior in various limits, and is consistent with previously reported experimental observations. Specifically, it predicts the formation of equilibrium intrusions when the intrusion density equals the depth-weighted mean density of the two ambient layers. It furthermore demonstrates the existence of non-smooth limits under certain conditions. An energy analysis shows that under non-equilibrium conditions the intrusion gains energy. The predictions by the parametric study are furthermore compared to two-dimensional DNS results, and very good agreement is observed with regard to all flow properties.

1. Introduction
Intrusions represent a special class of gravity currents that propagate horizontally into a stratified ambient at intermediate depths. They occur in a variety of atmospheric and oceanic situations, where they can influence the dynamics of such flows as sea breeze fronts, river plumes and powder snow avalanches.
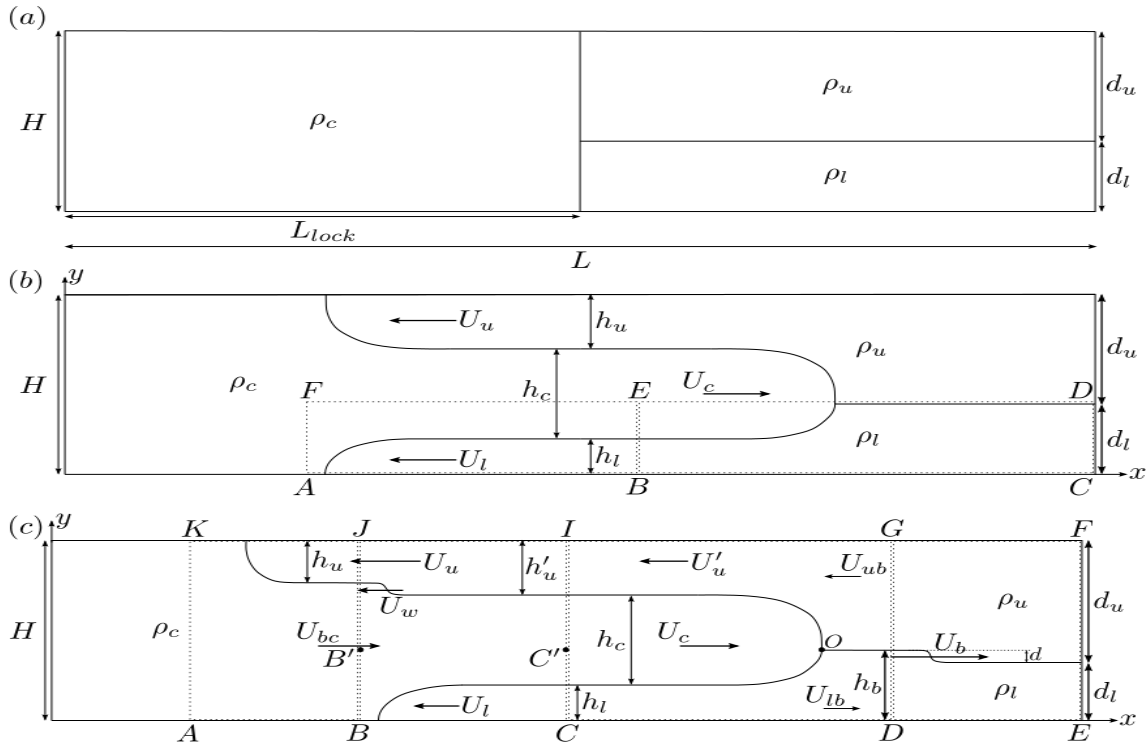

Fig1. Schematic of an intrusion produced via a lock-release process: a) at the initial state, where all the fluids are at rest, b) when the gate is removed and a quasisteady, symmetric intrusion forms and c) when $(\rho_l d_l + \rho_u d_u)/H < \rho_c$ and a quasisteady, non-symmetric intrusion emerges.

The most common way to produce the intrusion in the laboratory is via lock-release process. The schematic of a lock-release has been sketched by figure 1a. A tank of length L and height H is divided into two compartments by means of a vertical gate. The right compartment is initially filled up to height d_l with heavy fluid of density ρ_l. A lighter fluid layer of density ρ_u and thickness d_u is placed above this dense fluid. The left compartment (the 'lock') of length L_{lock} contains fluid of intermediate density ρ_c, so that $\rho_u < \rho_c < \rho_l$. Upon instantaneous removal of the gate, the intermediate density fluid forms a right-propagating intrusion, while two left-propagating currents emerge as the consequence of return flows. This fully describes the schematic of a *symmetric* or *equilibrium intrusion*, exhibited by figure 1b, where ρ_c equals average density of ambient fluids, weighted by their depths $(\rho_c d_l + \rho_c d_u)/H$. As soon as this symmetry or equilibrium condition breaks, the *non-symmetric* or *non-equilibrium* intrusion will form, which gives rise to the leading bore propagating ahead of the intrusion, as well as the substantial difference in the velocities of the left-propagating currents. This velocity difference results in the generation of another bore, travelling along the interface of the faster left-propagating current, always at the same streamwise location as the slower one. Figure 1c represents this dynamics.

Various theoretical models have been proposed to predict the features of the intrusions, such as their thickness and front velocity ([1], [2], [3], [4]). Unanimously, all these earlier models are based on some form of empirical energy assumptions, e.g. they may assume zero-headloss along certain streamlines, while they employ mass and horizontal momentum conservation equations ([1], [2], [4]), or they consider non-dissipative conversion of all the available potential energy to kinetic energy of the intrusion and return flows, in the absence of mixing ([3]). In the present investigation, we aim to avoid such empirical assumptions, by using horizontal and vertical momentum conservation simultaneously in the form of vorticity equations, in addition to the mass conservation equations. It allows us to analyze the energetics of the flow *a posteriori*.

2. Theory & simulations

The simultaneous application of the mass and vorticity conservation equations on the symmetric and non-symmetric configurations shown in figure 1b and 1c, respectively, and for the separate control volumes exhibited for each configuration, yields the flow variables, particularly gravity current speeds and thicknesses, without invoking any empirical assumptions for the closure. The details of the theoretical analysis can be found in [5]. The results of the analytical solution can be rendered dimensionless, by introducing H and $\sqrt{g'H}$ as the characteristic length and velocity, respectively. Here, g' is defined as $(\rho_l - \rho_u)g/\rho_c$. Moreover, a dimensionless density can be formulated as $\rho^* = (\rho - \rho_u)/(\rho_l - \rho_u)$. Consequently, the equilibrium condition in the dimensionless form gives $\rho_c^* = d_l^*$.

This vorticity model predicts identical velocities for all the gravity currents in the symmetric case, where they all equal $\sqrt{d_l^* d_u^*}/2$. Furthermore, it shows that the effective depths of each left-propagating currents is half the depth of the corresponding layer, i.e. $h_l^* = d_l^*/2$ and $h_u^* = d_u^*/2$. These results are fully consistent with [1], [2], [3] and [4]. For the non-symmetric intrusion, a closed-form solution is not attainable, due to the complexity and the nonlinearity of the system of the equations, but a numerical solution can be obtained via Newton iteration or other numerical methods.

Toward verifying the validity of the analytical solution, the results obtained by the above theory, were compared with the earlier theoretical and experimental data, as well as with the results of two-dimensional and unsteady Direct Navier-Stokes Simulations (DNS) provided by the in-house code TURBINS, which has been described and validated in [6] and [7]. The dynamics of various types of intrusions introduced earlier in this paper, are captured in figure 2. Doubly symmetric intrusion refers to the special case of symmetric intrusion where $\rho_c = (\rho_l + \rho_u)/2$ and $d_l = d_u$. In this case, there is a complete symmetry with respect to the ambient interface.
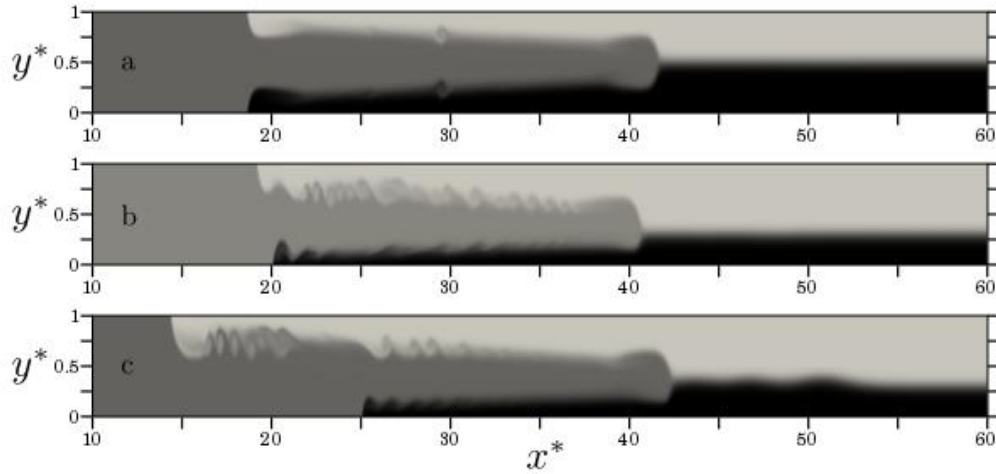
Fig 2. Snapshots of the density field of a) a doubly symmetric, b) a symmetric, and c) a non-symmetric intrusion, when the numerical solutions have reached the quasisteady state.

3. Results

In the following, we conduct a comprehensive comparison between the present vorticity-based modelling and previous experimental or theoretical studies, in addition to the results obtained through DNS.
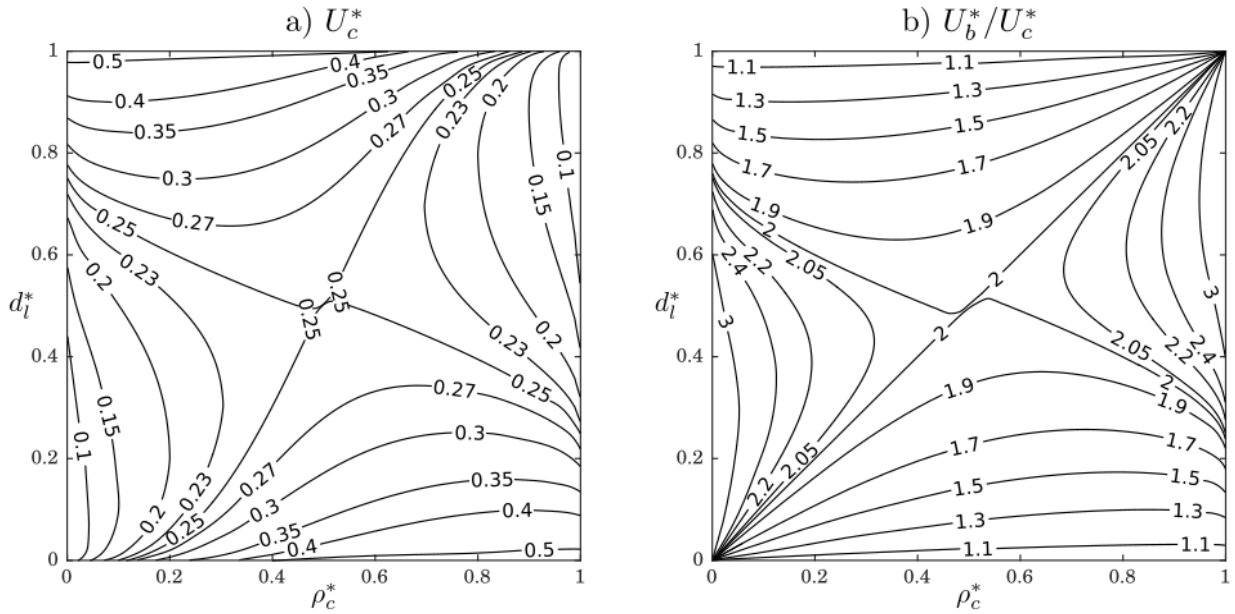

Fig 3. Phase-space diagrams for a) the intrusion speed, and b) the ratio of leading wave speed to intrusion speed.

Presenting the results of our model in the form of contours and as functions of ρ_c^* and d_l^* is informative. For instance, figure 2 represents the phase-space diagrams for the intrusion speed, as well as the ratio of leading wave speed to intrusion speed for the full range of dimensionless intrusion densities and interface heights. The model confirms that for a given intrusion density, equilibrium intrusions have the minimum speed. For this reason, in figure 1a, the extrema of all the isolines pass through line $\rho_c^* = d_l^*$. Furthermore, at $\rho_c^* = d_l^* = 0.5$, where the doubly symmetric intrusion forms, the vorticity model renders the same prediction as the classical studies on single-layer gravity current such as [8], when the

tank height equals $H/2$. Figure 2b illustrates that for symmetric intrusions $U_b^*/U_c^* = 2$, so that the correct linear long wave speed $\sqrt{d_l^* d_u^*}$ is achieved, which is in agreement with [2] and [4]. It is also noteworthy that for the limiting cases, where d_l^* approaches 0 or 1, the ratio of intrusion speed to the leading wave speed tends to 1, i.e. the intrusion catches up with the leading bore. This is consistent with the fact that for these limits, the single-layer gravity current case will be recovered, where we do not expect the emergence of any internal bore.
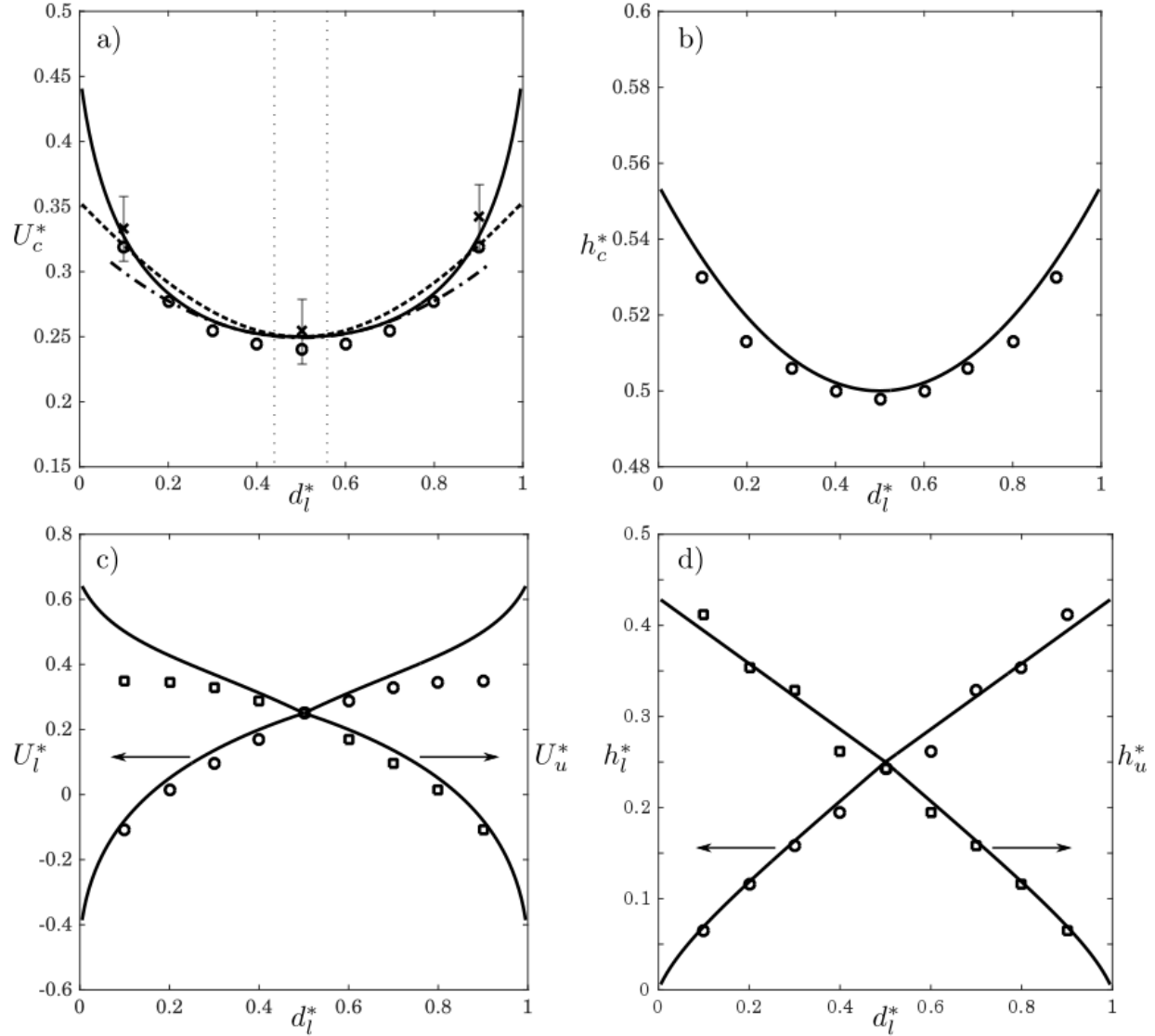

Fig 4. Variation of a) the intrusion speed (U_c^*), b) intrusion thickness (h_c^*), c) left-propagating current velocities (U_l^*, U_u^*) and d) left-propagating current heights (h_l^*, h_u^*) as functions of d_l^*, when ρ_c^* is maintained at 0.5. The solid lines demonstrate the results of the present study, dashed line exhibits the predictions of [3], dash-dot line displays the results presented by [4] and discrete circles and crosses show the DNS results of the present study and the experimental data of [3], respectively. Furthermore, the vertical dotted lines in 4a demonstrate the range of validity of the investigation by [1]. Within this range, their results (not shown here) agree closely with all other theoretical, numerical and experimental data.

The results can also be studied for a fixed value of ρ_c^*, such as those shown in figure 4. For the intrusion velocity, figure 4a compares vorticity model predictions with current DNS simulation results, as

well as with earlier experimental data and theoretical predictions by other authors. Within the present investigation, we conducted simulations for $d_l^* = 0.1$, 0.2...0.9, as well as various ρ_c^*-values, while only those of $\rho_c^* = 0.5$ are presented here. The figure shows that the vorticity model predictions are close to those of the earlier models by [3] and [4], and over a remarkable range of d_l^* fall in between these two models. Within its narrow range of validity between the vertical dotted lines, the model of [5] yields predictions in very close agreement with those of the other models, so that we do not show them in this figure. All four models predict that the minimum propagation velocity occurs at equilibrium conditions, which is consistent with the experimental observations of [7] and the present simulation results. Due to the finite Re-values employed in the DNS simulations, the DNS front velocity data generally fall slightly below the vorticity model predictions. We note that in the limit of $d_l^* \rightarrow \rho_c^*$, the predictions for the non-symmetric case smoothly approach those of the symmetric case for all physical variables.

Figure 4b compares vorticity model predictions with DNS results for h_c^* as a function of the interface height. As shown clearly, the intrusion thickness reaches a minimum value of 0.5 for the equilibrium case. Away from the equilibrium point, the intrusion thickens. This can be explained clearly via studying the energetics of the flow, as will be seen later.

For the propagation velocities of the upper and lower gravity currents, figure 4c compares the vorticity model predictions to the DNS results. Again, good overall agreement is observed, particularly away from the limits. The velocity of each gravity current is a function of its available potential energy, which scales with the square of the layer height multiplied by its density difference relative to the intrusion fluid. Both the model predictions and the DNS results confirm that under equilibrium conditions ($\rho_c^* = d_l^*$) the gravity currents have identical front velocities. When $d_l^* < \rho_c^*$, the lower gravity current has less available energy than the upper one, so that it travels more slowly. As d_l^* increases, the lower gravity current speeds up while the upper one slows down, until for $\rho_c^* = d_l^*$ the two velocities become equal to each other. Beyond this point, the lower gravity current propagates faster than the upper one. We notice that for $d_l^* \approx 0$ or 1 the vorticity model predicts velocity of the faster left-propagating current above 0.6. This is much larger than the value of one half for a full-depth lock-exchange gravity current, which indicates that the limits of $d_l^* \rightarrow 0$ and 1 are singular. This singularity may be a consequence of treating the interfacial disturbances as a bore, which is no longer valid for these limiting cases. An alternative approach could be to model these disturbances as solitary waves, which represents a substantially different dynamics from that of a bore. It furthermore suggests that in this limit the lower gravity current in the intrusion configuration is gaining energy.

Figure 4d compares the DNS values for the lower and upper current heights with the corresponding vorticity model predictions. Again, good agreement between the model predictions and the simulation results is observed over the entire range of d_l^*, for the exhibited values of ρ_c^*. Moreover, as demonstrated by this figure, h_l^* and h_u^* vary nearly linearly with the interface height, especially far from $d_l^* = 0$ or $d_l^* = 1$, where the slopes of the curves are close to 0.5 (and -0.5 for h_u^*). Recall that for equilibrium intrusions we had found $h_l^* = d_l^*/2$ and $h_u^* = d_u^*/2$.
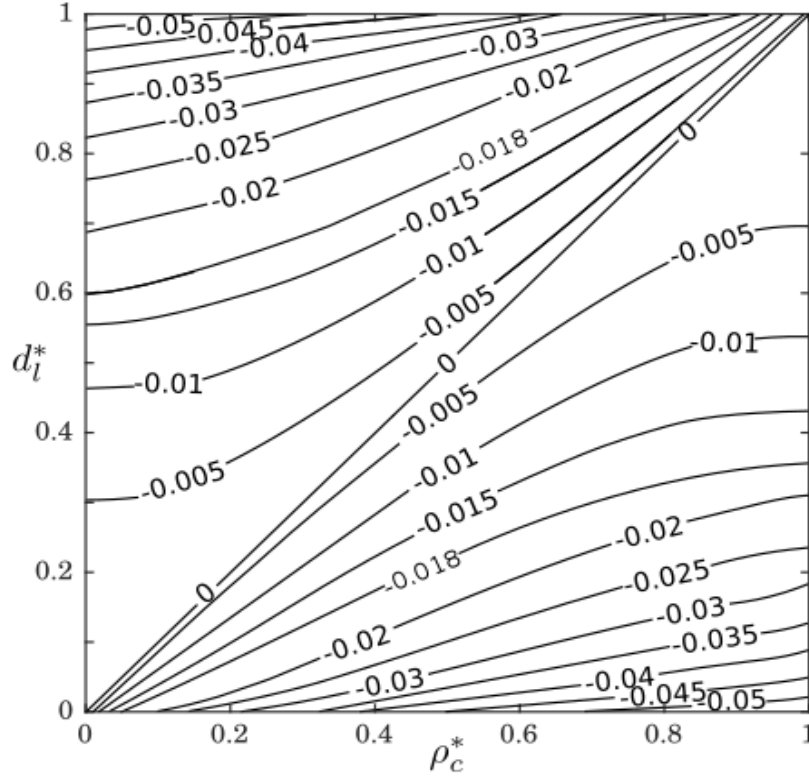
Fig 3. Phase-space diagram the headloss (Δ_c^*) along $B'C'$ streamline and within the intrusion.

After obtaining the velocity and thickness of each gravity current theoretically, we can also compute the headloss Δ_c^* along the streamline $B'C'$ shown in figure 1c via employing modified Bernoulli's equation between these two points. Pressure is assumed to be hydrostatic at the two ends of this streamline. We also note that the headloss is scaled by $\rho_c g'H$. Interestingly, it yields zero dissipation for the symmetric intrusions, which is consistent with the fact that intrusion occupies half the depth of the tank in these cases. This result also agrees well with [8], which shows that an energy-conserving gravity current forms only when its thickness is either zero or half the depth of the tank. On the other hand, away from the equilibrium condition, Δ_c^* is always negative, i.e. the intrusion gains energy. This explains the propagation of non-equilibrium intrusions with $h_c > H/2$.

References
[1] J. Y. Holyer and H. E. Huppert, 1980, *J. Fluid Mech* vol. 100, 739-767.
[2] B. R. Sutherland, P. J. Kyba and M. R. Flynn, 2004, *J. Fluid Mech.* vol.514, 327-353.
[3] H. -B. Cheong, J. J. P. Kuenen and P. F. Linden, 2006, *J. Fluid Mech.* vol. 552, 1-11.
[4] M. R. Flynn and P. F. Linden, 2006, *J. Fluid Mech.* vol. 568, 193-202.
[5] M. A. Khodkar, M. M. Nasr-Azadani, 2016, Submitted to *Physical Review Fluids.*
[6] M. M. Nasr-Azadani and E. Meiburg, 2011*, Computers & Fluids vol. 45,* 14-28*.*
[7] M. M. Nasr-Azadani H. Ball and E. Meiburg, 2013*, Computers & Geosciences vol. 45,* 141-153*.*
[8] T. B. Benjamin, 1968, *J. Fluid Mech.* vol. 31, 209-248.